STEM CELLS
TRANSLATIONAL MEDICINE®

Intracarotid Infusion of Mesenchymal Stem Cells in an Animal Model of Parkinson's Disease, Focusing on Cell Distribution and Neuroprotective and Behavioral Effects

SILVIA CERRI,[a] ROSARIA GRECO,[b] GIOVANNA LEVANDIS,[a] CRISTINA GHEZZI,[a]
ANTONINA STEFANIA MANGIONE,[b] MARIE-THERESE FUZZATI-ARMENTERO,[a] ARIANNA BONIZZI,[a]
MARIA ANTONIETTA AVANZINI,[c] RITA MACCARIO,[c] FABIO BLANDINI[a]

[a]Laboratory of Functional Neurochemistry, Center for Research in Neurodegenerative Diseases, and [b]Laboratory of Neurophysiology of Integrative Autonomic Systems, "C. Mondino" National Neurological Institute, Pavia, Italy; [c]Immunology and Transplantation Laboratory/Cell Factory/Pediatric Hematology/Oncology Department, Fondazione IRCCS Policlinico San Matteo, Pavia, Italy

Correspondence: Fabio Blandini, M.D., Ph.D., Laboratory of Functional Neurochemistry, Center for Research in Neurodegenerative Diseases, "C. Mondino" National Neurological Institute, via Mondino 2, 27100, Pavia, Italy. Telephone: 39-0382-380416; E-Mail: fabio.blandini@mondino.it

ABSTRACT

Mesenchymal stem cells (MSCs) have been proposed as a potential therapeutic tool for Parkinson's disease (PD) and systemic administration of these cells has been tested in preclinical and clinical studies. However, no information on survival and actual capacity of MSCs to reach the brain has been provided. In this study, we evaluated homing of intraarterially infused rat MSCs (rMSCs) in the brain of rats bearing a 6-hydroxydopamine (6-OHDA)-induced lesion of the nigrostriatal tract, to establish whether the toxin-induced damage is sufficient to grant MSC passage across the blood-brain barrier (BBB) or if a transient BBB disruption is necessary. The rMSC distribution in peripheral organs and the effects of cell infusion on neurodegenerative process and motor deficits were also investigated. rMSCs were infused 14 days after 6-OHDA injection. A hyperosmolar solution of mannitol was used to transiently permeabilize the BBB. Behavioral impairment was assessed by adjusting step test and response to apomorphine. Animals were sacrificed 7 and 28 days after cell infusion. Our work shows that appreciable delivery of rMSCs to the brain of 6-OHDA-lesioned animals can be obtained only after mannitol pretreatment. A notable percentage of infused cells accumulated in peripheral organs. Infusion of rMSCs did not modify the progression of 6-OHDA-induced damage or the motor impairment at the stepping test, but induced progressive normalization of the pathological response (contralateral turning) to apomorphine administration. These findings suggest that many aspects should be further investigated before considering any translation of MSC systemic administration into the clinical setting for PD treatment. STEM CELLS TRANSLATIONAL MEDICINE 2015;4:1–13

SIGNIFICANCE

This study demonstrates that mesenchymal stem cells infused through the carotid artery do not efficiently cross the blood-brain barrier in rats with a Parkinson's disease-like degeneration of nigrostriatal neurons, unless a permeabilizing agent (e.g., mannitol) is used. The infusion did not reduce the neuronal damage and associated motor impairment, but abolished the motor abnormalities these animals typically show when challenged with a dopaminergic agonist. Therefore, although arterially infused mesenchymal stem cells did not show neurorestorative effects in this study's Parkinson's disease model, they appeared to normalize the pathological responsiveness of striatal neurons to dopaminergic stimulation. This capability should be further explored in future studies.

INTRODUCTION

Neurorestorative cell-based therapies have been repeatedly proposed for Parkinson's disease (PD) since the late 1980s, when the first striatal grafts of ventral mesencephalon dopaminergic cells were attempted in PD patients [1–4]. More recently, stem cells have been proposed as a promising tool to achieve neurorestoration in the PD brain. Numerous studies have been conducted in PD animal models, with different stem cell types, including embryonic [5–7] or adult neural stem cells [8], dopaminergic cells differentiated from fibroblast-derived inducible pluripotent stem (iPS) cells [9–11] and bone marrow- and adipose-derived mesenchymal stem cells (MSCs) [12–22]. Most of the cell types tested in PD models proved able, with variable degrees of efficiency, to counteract nigrostriatal neurodegeneration and associated

motor abnormalities. MSCs, in particular, have attracted considerable interest for a number of peculiar features. MSCs can be easily derived and expanded from bone marrow aspirates [23] and show negligible oncogenic potential [24–28]. Compared with embryonic or iPS cells, MSCs are less prone to differentiate toward the neuronal phenotype; on the other hand, MSCs possess remarkable immunomodulatory, neurotrophic, and neurogenic properties [29–34].

MSCs are the only stem cells tested, so far, in patients with degenerative parkinsonism. Results have been published from two open-label studies in PD patients [35, 36] and two studies (an open-label and a double-blind, randomized clinical trial) in patients with multiple system atrophy (MSA), a form of atypical neurodegenerative parkinsonism characterized by multiple neuronal lesions [37, 38]. An additional open-label study was conducted in PD patients treated with bone marrow-derived hematopoietic (CD34+) cells [39]. In these studies, different routes of administration were tested. In fact, whereas in the studies of Venkataramana et al. [35, 36], MSCs were stereotaxically injected into the lateral ventricles, in the other studies, a systemic (intra-arterial or intra-arterial plus intravenous) route was chosen [37–39]. These studies suggested that systemic administration of MSCs is safe and grants a modest reduction of disease severity and a delayed progression of neurological deficits. However, no information was provided on the survival of infused MSCs, efficiency of MSC homing within the brain, or invasion of peripheral organs by infused cells. Very little information on these aspects is available, even in experimental PD models.

The first aim of our study was to assess homing of intraarterially infused MSCs in the brain of rats bearing a 6-hydroxydopamine (6-OHDA)-induced lesion of nigrostriatal neurons, a classic toxic model of PD, to establish whether the toxin-induced damage is sufficient to grant MSCs passage across the blood-brain barrier (BBB) or if a transient BBB disruption is necessary. In fact, 6-OHDA injection into the nigrostriatal tract moderately increases BBB permeability at the sites of neuronal damage [40]; analogously, in PD patients, slight BBB alterations may occur, particularly in the advanced stages of the disease [41, 42], but whether these alterations are sufficient to let MSCs pass through the BBB is unknown. On the other hand, it is known that mannitol, an osmotic agent approved for use in humans, transiently disrupts the BBB and, for this reason, is used to improve delivery of chemotherapeutic agents to the brain in patients with cerebral tumors [43]. In rats with experimentally induced intracerebral hemorrhage [44] or traumatic brain injury [45], pretreatment with mannitol substantially improved the passage of intraarterially infused bone marrow-derived stem cells into the brain parenchyma. In parallel to the cerebral distribution of MSCs after intracarotid infusion, we investigated the invasion of peripheral organs. Finally, we examined the effects of intraarterial infusion of MSCs on the progression of nigrostriatal degeneration and motor deficits induced by 6-OHDA injection.

MATERIALS AND METHODS

Animals

Male Wistar rats (200–225 g; Charles River, Calco, LC, Italy, http://www.criver.com) were housed two per cage, at 20°C–22°C on a 12-hour light-dark cycle, with food and water ad libitum at the Centralized Animal Facility of the University of Pavia. All procedures were in accordance with the European Convention for Care and Use of Laboratory Animals and were approved by the local animal ethics committee of the University of Pavia.

Experimental Design

A first set of preliminary experiments was conducted to verify the efficacy of the transient, mannitol-induced BBB disruption procedure. To this purpose, 14 days after 6-OHDA intrastriatal injection, Evans Blue extravasation in the brain, a measure of BBB permeability, was evaluated in animals randomly assigned to pretreatment with mannitol or saline (four per group).

Following preliminary experiments, we evaluated: (a) the biodistribution of rat MSCs (rMSCs) after intracarotid infusion and (b) the effect of rMSC infusion on the progression of nigrostriatal degeneration and motor deficits induced by 6-OHDA injection. Fourteen days after 6-OHDA or saline (sham or unlesioned animals) intrastriatal injection, animals (eight per group) were randomly assigned to the following experimental groups: (a) intracarotid infusion of rMSCs preceded by transient BBB disruption; (b) intracarotid infusion of saline/heparin preceded by transient BBB disruption; and (c) intracarotid infusion of rMSCs in the absence of transient BBB disruption.

Behavioral tests were performed at different time points during the entire experimental period (as described below). Animals were then sacrificed 7 or 28 days after infusion of rMSCs or saline/heparin (Fig. 1).

The time of rMSC infusion was chosen according to the features of the PD model used in our study where the intrastriatal 6-OHDA injection causes a retrograde nigrostriatal degeneration that, at the 14th day, is still evolving, thereby resembling the slowly evolving nature of the nigrostriatal degeneration in human PD [46].

Isolation, Culture, and Characterization of rMSCs

MSCs were isolated from bone marrow stromal cells collected from femurs and tibias of male Wistar rats 6–8 weeks old. Cell suspensions were filtered, then centrifuged for 7 minutes at 200g. Pellets were resuspended and cultured in complete growth medium (Dulbecco's Modified Eagle Medium containing 20% fetal bovine serum and 1% penicillin-streptomycin mixture) at 37°C, 90% humidity, and 5% carbon dioxide in air. When the colonies became evident, cells were detached with trypsin, counted, and plated (200,000 cells per T75 flask). After the third passage, cell surface markers were analyzed to determine purity of the rMSC population. Adherent cells were trypsinized, harvested, and incubated with Thy1, CD29, CD49e (positive), and CD11b, CD45 (negative) antibodies. The recommended isotype controls for each fluorochrome were also adopted (BioLegend, San Diego, CA, http://www.biolegend.com; Lifespan Biosciences, Seattle, WA, http://www.lsbio.com). After incubation, cells were washed with phosphate-buffered saline and analyzed on a Navios Flow Cytometer (Beckman Coulter, Miami, FL, http://www.beckmancoulter.com) equipped with Kaluza software.

In parallel, immunocytochemistry was performed using a panel of positive (Thy1, CD29) and negative (CD11b, CD45) MSC markers. The following primary antibodies and dilutions were used in this study: rabbit anti-Thy1 (1:100; Abcam, Cambridge, U.K., http://www.abcam.com), rabbit anti-CD29 (1:500; Millipore, Billerica, MA, http://www.emdmillipore.com), mouse anti-CD11b (1:300; Serotec, Oxford, U.K., http://www.abdserotec.com), and mouse anti-CD45 (1:100; Millipore). Negative immunofluorescent controls were performed using a mouse IgG or a rabbit IgG (Millipore) instead of the primary antibody.
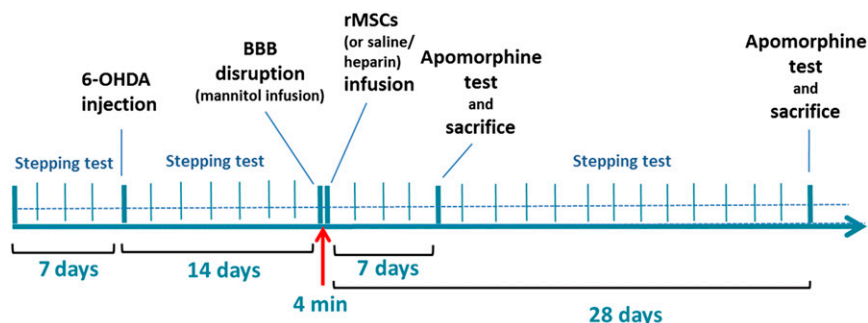
Figure 1. Experimental design. Fourteen days after stereotaxic injection of 6-OHDA into the striatum, animals had undergone rMSCs or saline/heparin infusion, preceded by transient blood-brain barrier (BBB) disruption procedure. Animals were sacrificed 7 or 28 days after infusion of cells (or saline/heparin). Stepping and apomorphine tests were performed during the entire course of the experiments and the day of the animal sacrifice, respectively. Abbreviations: 6-OHDA, 6-hydroxydopamine; BBB, blood-brain barrier; rMSC, rat mesenchymal stem cell.

Surgical Procedures

6-OHDA Stereotaxic Injection

Animals were anesthetized by i.p. administration of 50 mg/kg of sodium-thiopental and placed in a stereotaxic frame (Stoelting, Wood Dale, IL, http://www.stoeltingco.com). They received an injection of 6-OHDA (20 μg per 3 μl in saline containing 0.02% ascorbic acid) (Sigma-Aldrich, St. Louis, MO, http://www.sigmaaldrich.com) or saline into the right striatum (1.0 mm anterior, 3.0 mm lateral, and 5.0 mm ventral with respect to bregma and dura) [47] at 1 μl/min, using a Hamilton 10-AL syringe with a 26-gauge needle.

Carotid Artery Surgery

Animals were anesthetized using Equithesin (3.6 ml/kg, i.p.) [48] and kept at 37°C with a heating pad during all surgical procedures (HB 101/2 RS; 2Biological Instruments, Varese, Italy, http://www.2biol.com). A catheter (PE-50 tubing, internal diameter: 0.58 mm; 2Biological Instruments) was inserted into the external carotid artery and gently advanced toward the bifurcation to reach the internal carotid artery (ICA). The catheter was secured with vascular clips (Micro-Serrefine; 2Biological Instruments) and used for the infusions of mannitol and/or rMSCs. A catheter was also placed into the right jugular vein of the subgroup of animals used for BBB permeability assessment.

Transient Blood-Brain Barrier Disruption

A BBB opening was achieved by infusing a hyperosmolar solution of mannitol (25%) into the ICA; the procedure increases vascular permeability with a peak at 5 minutes postinfusion [49, 50]. The mannitol solution was heated to 37°C before infusion, to prevent crystallization, and infused at a constant rate of 0.12 ml/s for 30 seconds [51].

Evans Blue Extravasation

To verify BBB permeability following hypertonic mannitol infusion, Evans Blue staining was performed in a subgroup of animals, according to the protocol described by Blanchette and Fortin [51]. Briefly, 2% Evans Blue solution (4 ml/kg), dissolved in 50% saline/50% heparin (600 IU/ml), was administered via the right jugular vein, 5 minutes before mannitol. Fifteen minutes later, animals were perfused by intracardiac infusion of 4% paraformaldehyde. Brains were removed and cut into 2-mm thick coronal slabs, using a brain matrix. Coronal slabs were postfixed for 48 hours and scanned to evaluate the extension of BBB

permeabilization, as indicated by the Evans Blue staining, by using ImageJ software (US National Institutes of Health, Bethesda, MD, http://imagej.nih.gov/ij). The stained volume was expressed as a percentage of the total volume of the ipsilateral hemisphere.

Rat MSC Labeling and Infusion

Fourteen days after the stereotaxic injections, 1×10^6 rMSCs were labeled, resuspended in 100 μl of 50% saline/50% heparin (600 IU/ml), and injected into the right ICA 4 minutes after the injection of mannitol or saline/heparin. Two dyes were used for cell labeling: a membrane-intercalating dye emitting in the near-IR 815-nm spectrum (CellVue NIR815 Kit for Membrane Labeling; Polyscience, Warrington, PA, http://www.polysciences.com) [52, 53] and lipophilic red fluorescence dye PKH26 (PKH26 Red Fluorescent Cell Linker Kits; Sigma-Aldrich) [54–57].

Behavioral Analyses

Adjusting Step Test

Forelimb akinesia associated with 6-OHDA-induced nigrostriatal damage was assessed using the adjusting step test. Following the original procedure described by Ollson et al. [58], the number of steps performed with the left paw (contralateral to the lesion side) was counted, both in the backhand and forehand directions, to adjust for the lateral movement imposed by the experimenter. Rats were evaluated the week before surgery, to accustom the animals to human manipulation (training phase) and to obtain a basal value. Postlesion testing, starting 1 day after the 6-OHDA/saline injection, was performed until the day of sacrifice, with the exception of the day after carotid surgery, to avoid further distress to animals. Each test consisted of three evaluations per day, performed three times per week.

Turning Behavior

Before being sacrificed, animals were tested with apomorphine (0.5 mg/kg in 0.1% ascorbic acid, i.p.; Sigma-Aldrich) to evaluate whether rMSC infusion modified the rotational response to this drug—a classic method to test dopaminergic denervation in rodents with unilateral nigrostriatal lesion. The number of complete turns performed by the animals in 45 minutes was measured with an automated rotometer (Ugo Basile, Comeria, VA, Italy, http://www.ugobasile.com).

Sacrifice and Ex Vivo Near-IR Imaging

Seven and 28 days after infusion of rMSCs or saline/heparin, animals were sacrificed by a lethal injection of sodium pentobarbital and perfused transcardially with cold saline solution followed by 4% paraformaldehyde. Brain and peripheral organs (lungs, spleen, liver, and kidneys) were excised and underwent near-IR (NIR) imaging using the Odyssey imager (Li-Cor Biosciences, Lincoln, NE, http://www.licor.com) to evaluate whole-body rMSC distribution.

Rat MSC Tracking in the Brain

Serial coronal sections (25 μm) of the brain were cut using a freezing sliding microtome (SM 2000R; Leica, Milan, Italy, http://www.leica-microsystems.com), mounted on slides, and dried at room temperature in the dark. Sections were then covered with Prolong with 4',6-diamidino-2-phenylindole (DAPI; Life Technologies, Grand Island, NY, http://www.lifetechnologies.com) and observed under a fluorescent Zeiss Apotome microscope (Carl Zeiss, Jena, Germany, http://www.zeiss.com). Rat MSCs, coexpressing NIR815 and PKH26, were counted in every four sections extending from 0.70 to 11.60 mm from bregma, in both hemispheres. Results represent the estimated absolute number of the rMSCs engrafted into the brain. The percentage of infused cells localized in the striatum and substantia nigra was also reported.

Immunohistochemical Analyses

Tyrosine hydroxylase (TH) immunohistochemical staining was performed on 40-μm free-floating sections to verify the loss of dopaminergic terminals and cell bodies in the striatum and substantia nigra pars compacta (SNc), respectively, as previously described [46]. The striatal dopaminergic terminal lesion was evaluated by considering the striatal volume deprived of TH staining. Briefly, both the entire striatal area and the nonlesioned area were measured in every fourth section throughout the whole rostrocaudal extension of the striatum (anteroposterior anatomical levels: +1.7–2.30 mm, with respect to bregma [47]). Respective volumes were obtained by summing areas and multiplying them by the intersectional distance (100 μm); results were expressed as the percentage of striatal volume displaying TH immunoreactivity with respect to the entire striatal volume. TH-positive cells in the SNc of both hemispheres were counted using stereological analysis (as described below).

Striatal c-Fos expression was detected by immunohistochemistry, as described previously [59]. C-Fos-positive cells of both lesioned and intact striatum were counted in five sections per animal and results were expressed as mean number of c-Fos-positive cells per mm². The "lesioned/nonlesioned side ratio" of striatal c-Fos expression was reported.

Stereological Count

Unbiased stereological count of dopaminergic cells in the SNc was made using the optical fractionator method [60] from the STEREO INVESTIGATOR program on a Neurolucida computer-controlled microscopy system (MBF Bioscience Inc., Williston, VT, http://www.mbfbioscience.com). TH-positive cells in the SNc of both lesioned and intact hemispheres were counted in every fourth section on comparable sections for all the subgroups of treatment, throughout the entire nucleus to evaluate neuronal survival.

Image Analysis

Immunohistochemical images were acquired with Zeiss Apotome and AxioVision software (Carl Zeiss). To visualize the near-IR signal, the microscope was further equipped with a Xenon arc lamps (N XBO 75; Carl Zeiss) and a filter for IR dye 800 (Chroma Technology Corp., Rockingham, VT, https://www.chroma.com).

Statistical Analysis

Comparisons between groups were carried out using the non-parametric Kruskal-Wallis test for evaluating differences in engraftment and the analysis of variance, followed by Tukey and Bonferroni post hoc tests for estimating variations of c-Fos expression and effects of rMSC infusion on behavioral analyses, respectively. A dedicated software (Prism 3 software; Graph-Pad Software, La Jolla, CA, http://www.graphpad.com) was used. The minimum level of statistical significance was set at $p < .05$.

RESULTS

Characterization of rMSCs

Flow cytometric analysis demonstrated that rMSCs were positive (>90%) for Thy1, CD29, and CD49e, and negative (<10%) for CD11b and CD45 (supplemental online Fig. 1A). Immunofluorescent labeling showed that rMSCs were positive for Thy1 and CD29, and negative for CD11b and CD45 (supplemental online Fig. 1B).

Effect of Mannitol on BBB Permeability

No Evans Blue extravasation was seen in the brain of 6-OHDA animals that did not receive mannitol (Fig. 2A). Conversely, after mannitol infusion, BBB permeability increased in the right hemisphere of 6-OHDA animals, as demonstrated by extravasation of plasma albumin bound to Evans Blue dye (Fig. 2B). Evans Blue staining extended along the entire rostrocaudal axis of the brain, with the exception of the cerebellum, and was visible in both cortical and subcortical areas, including the striatum. Quantitative analysis revealed a 42% increase in BBB permeability in the right hemisphere of rats pretreated with mannitol (Fig. 2C).

Effect of rMSC Infusion on Forelimb Akinesia

One week after the intrastriatal injection of 6-OHDA, all lesioned animals showed a marked decrease in the number of steps made by the paw contralateral to the lesioned hemisphere, compared with baseline values (Fig. 3A). Such decrease was not modified by rMSC infusion. Cell infusion per se had no effect on motor performance in unlesioned animals.

Effect of rMSC Infusion on Apomorphine-Induced Rotational Behavior and Striatal c-Fos Expression

Lesioned animals that received saline/heparin instead of rMSCs showed significant rotational response to apomorphine, contralateral to the lesioned side, at 1 and 4 weeks after the infusion procedure (Fig. 3B). Conversely, the contralateral rotational response was completely abolished in the lesioned animals that received the rMSCs infusion. In fact, these animals showed a moderate, yet significant, ipsilateral rotational response to apomorphine at the first week postinfusion; at the fourth week, even this ipsilateral rotational response to apomorphine subsided.
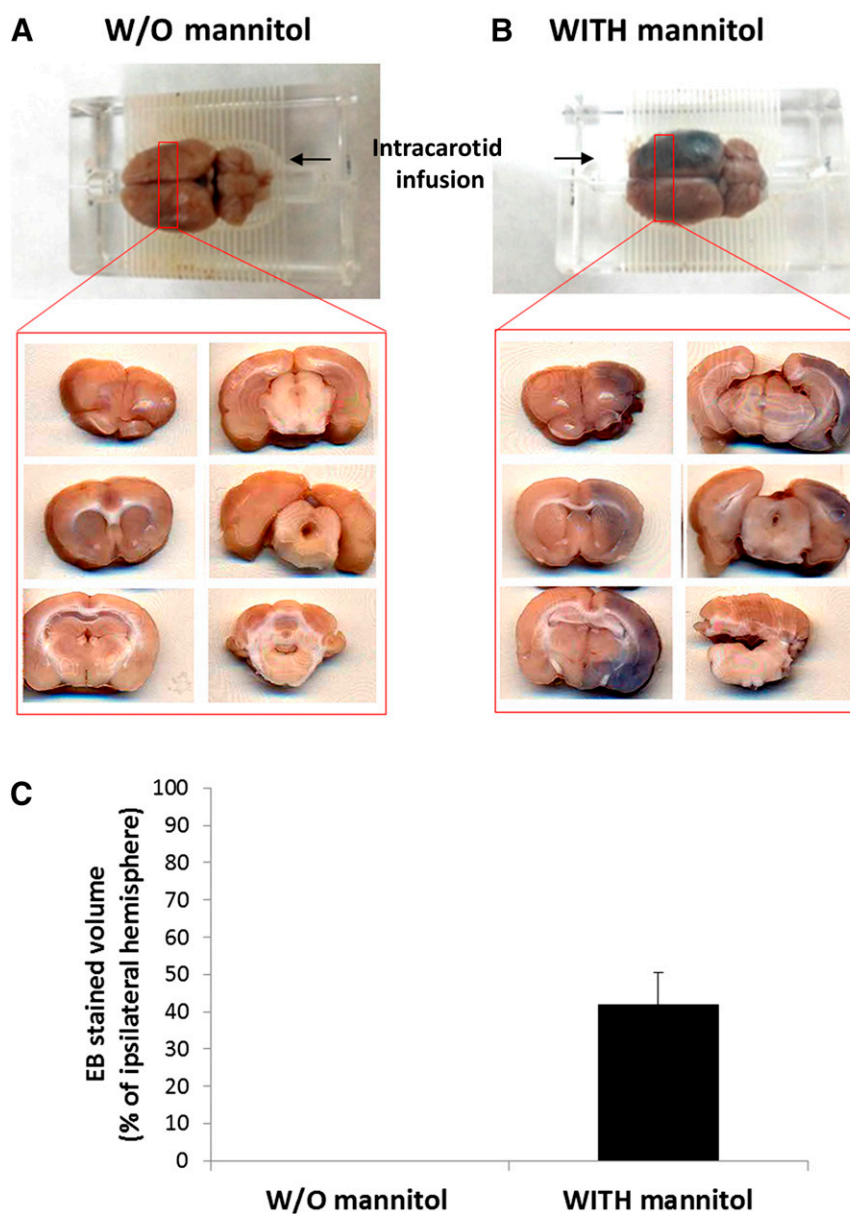
Figure 2. Effect of mannitol on BBB permeability in the intrastriatal 6-hydroxydopamine rat model. Representative photomicrographs of brain coronal sections showing Evans Blue extravasation in animals **(A)** W/O and **(B)** with 25% mannitol pretreatment. The right hemisphere (ipsilateral to intracarotid infusion) was strongly stained by EB dye in the rats receiving mannitol. **(C):** The administration of mannitol resulted in increased (42%) BBB permeability. Results (mean ± SEM) indicate the percentage of stained volume compared with the total volume of the ipsilateral hemisphere. Abbreviations: BBB, blood-brain barrier; EB, Evans Blue; W/O, without.

sham animals that received rMSCs did not show any relevant rotational response to apomorphine injection.

The rotational response to apomorphine of lesioned animals that did not receive rMSCs was associated with marked c-Fos expression in the denervated striatum and a low number of c-Fos-positive nuclei in the intact striatum (supplemental online Fig. 2). In lesioned rats that received the rMSC infusion, disappearance of the apomorphine-induced contralateral turning was associated with a remarkable increase in c-Fos expression in the intact striatum, while the number of c-Fos-positive nuclei in the denervated striatum remained unmodified. Sham animals that received rMSCs displayed a negligible number of c-Fos-positive nuclei in the striatum of both sides after

apomorphine. Overall, we observed that the lesioned/nonlesioned side ratio of striatal c-Fos expression was significantly reduced in 6-OHDA-lesioned rats receiving rMSCs compared with untreated animals.

Analysis of 6-OHDA-Induced Lesions

TH immunohistochemistry revealed that the intracarotid infusion of rMSCs did not affect the course of the 6-OHDA-induced neurodegeneration, either 1 or 4 weeks after the treatment. In fact, similar levels of survival of striatal TH-positive terminals (Fig. 4A, 4B) and SNc cell bodies (Fig. 4C–4E) were found in rMSC-treated and rMSC-untreated animals. Infusion of rMSCs per se did not alter
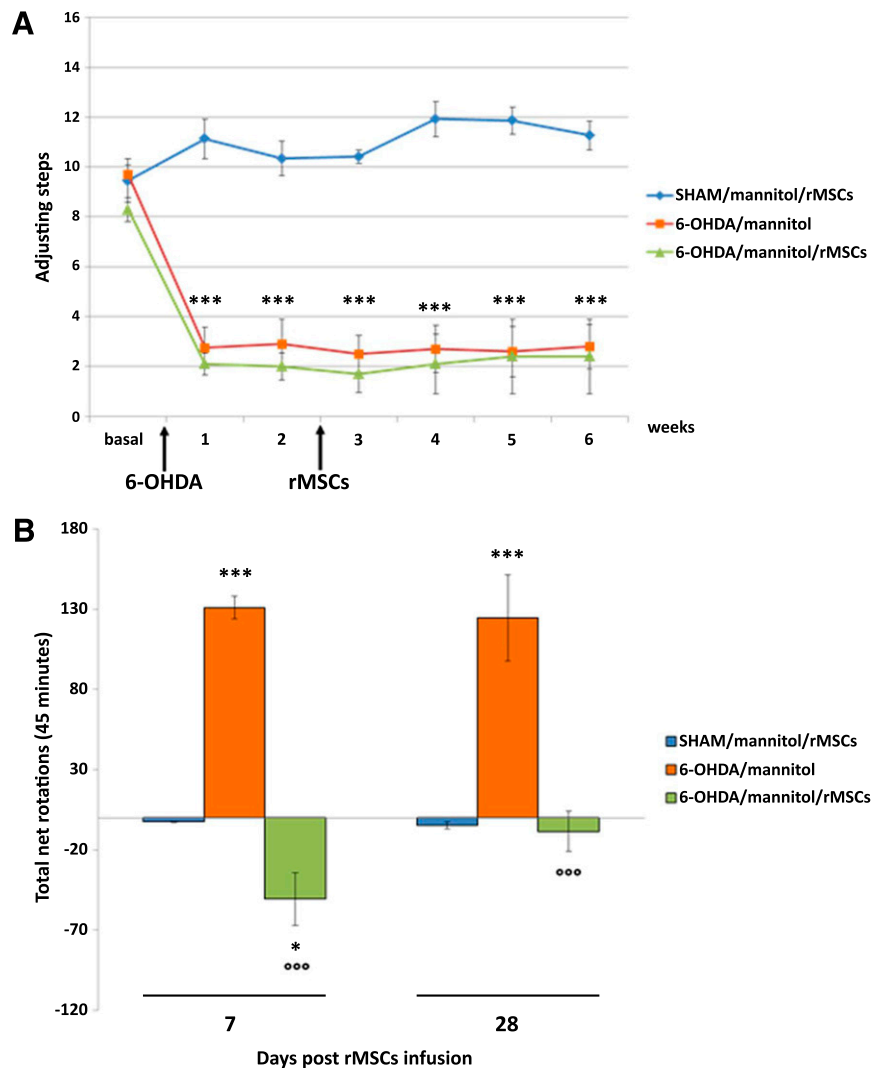
Figure 3. Effect of rMSC infusion on motor deficits and apomorphine-induced rotational behavior. **(A):** All 6-OHDA animals exhibited a decline in motor performance after the lesion. The infusion of rMSCs did not improve the motor deficits induced by 6-OHDA injection. Cell infusion per se had no effect on motor performance in sham animals. Results (mean $\pm$ SEM) indicate the average number of adjusting steps of the contralateral paw in the "forehand step" direction, carried out by animals during the 6 weeks of behavioral testing. Two-way ANOVA (time) F = 7.754, $p < .0001$, (treatment) F = 160.0, $p < .0001$; $***$, $p < .001$ Bonferroni post hoc test versus sham/mannitol/rMSCs (weeks 1–6, for both 6-OHDA groups). **(B):** Lesioned animals that did not receive rMSC transplantation exhibited a remarkable contralateral behavior after apomorphine administration, both 1 and 4 weeks after infusion procedure. Conversely, moderate ipsilateral turning in response to dopaminergic stimulation was observed in the group that received rMSCs 7 days after rMSC administration; no rotational response was observed 28 days post-rMSC infusion. No turning behavior was detected in unlesioned, transplanted animals. Bars represent the mean ($\pm$ SEM) number of total net rotations (contralateral minus ipsilateral rotations) performed by the animals in 45 minutes. Two-way ANOVA (time) F = 0.9739, $p = .3316$; (treatment) F = 70.72, $p < .0001$; Bonferroni post hoc test (7 and 28 days after rMSCs infusion). $*$, $p < .05$, $***$, $p < .001$ versus sham/mannitol/rMSCs; $°°°$, $p < .001$ versus 6-OHDA/mannitol. Abbreviations: 6-OHDA, 6-hydroxydopamine; ANOVA, analysis of variance; rMSC, rat mesenchymal stem cell; SHAM, unlesioned.

neuronal morphology or cytoarchitecture within the nigrostriatal tract, as verified by Nissl staining (data not shown).

Distribution of Infused rMSCs

No notable NIR signal (bright green) was detected after rMSC administration in the brains of 6-OHDA animals that did not receive mannitol infusion (Fig. 5A). Conversely, after mannitol pretreatment, a speckled near-infrared 815-nm (NIR815)-positive signal (Fig. 5B, arrowhead) was visible within the brain parenchyma, ipsilateral to the intracarotid infusion, indicating the presence of rMSCs 7 days after infusion. A quenched NIR signal was still observable 28 days following cell administration (data

not shown). Animals that did not receive rMSCs did not show any fluorescent labeling (Fig. 5C).

No relevant differences in the peripheral distribution of rMSCs were found between 7 and 28 days after infusion; therefore, the results discussed below are typical of both time points. Substantial NIR fluorescence was detected in the lungs and spleen of 6-OHDA rats receiving rMSCs, both with (Fig. 5B) and without (Fig. 5A) mannitol pretreatment. Conversely, a bright green signal was totally absent in the liver and kidneys (data not shown). No NIR signal was detected in peripheral organs of animals that did not receive the rMSC infusion (Fig. 5C).
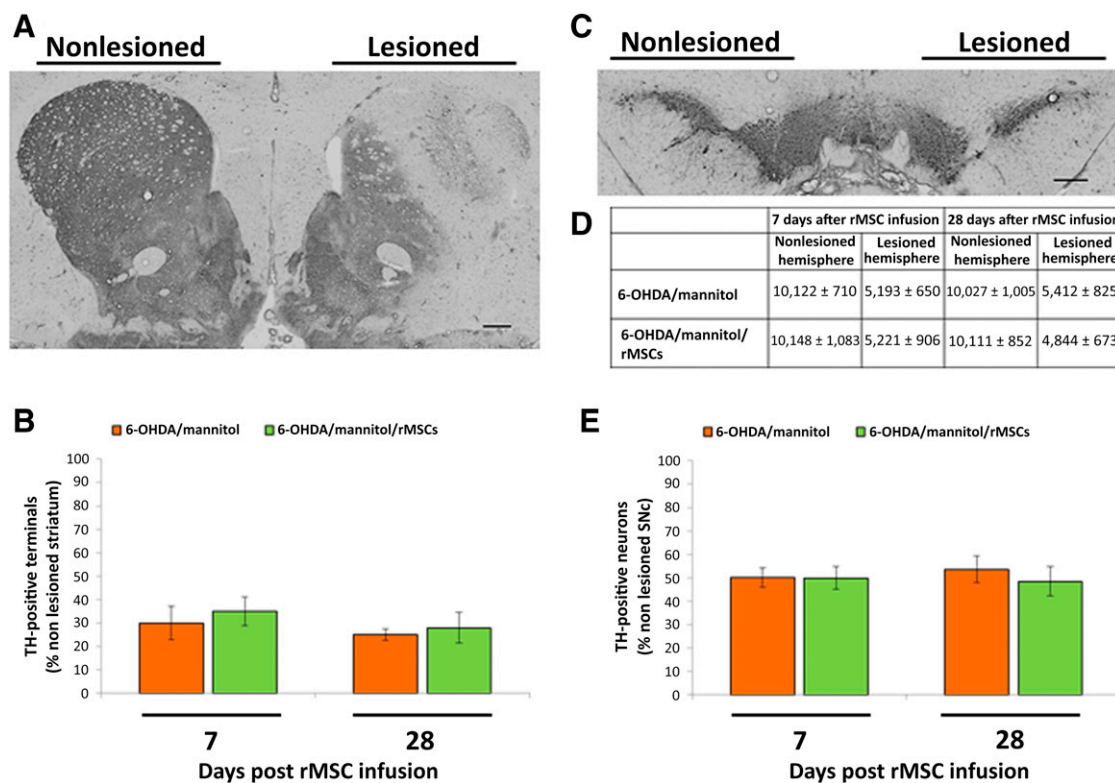
Published Ahead of Print on July 21, 2015 as 10.5966/sctm.2015-0023.

Cerri, Greco, Levandis et al.
7

Figure 4. Evaluation of 6-OHDA-induced nigrostriatal neurodegeneration. The intracarotid infusion of rMSCs did not affect the extent of 6-OHDA-induced neurodegeneration both in the short term (7 days) and long term (28 days) after infusion. **(A):** Representative photomicrographs of brain coronal sections showing striatal TH-positive terminals in both hemispheres. Scale bar: 500 μm. **(B):** Results (mean ± SEM) indicate the percentage of TH expression in the right striatum (injected with 6-OHDA) compared with the left, unlesioned striatum of rats that received an rMSCs infusion or saline/heparin. **(C):** Representative photomicrographs of brain coronal sections showing TH-positive cells of the SNc of both hemispheres. Scale bar: 500 μm. **(D, E):** Stereological counts of dopaminergic neurons in the SNc of rats that received an rMSCs infusion or saline/heparin. The number of dopaminergic neurons in the SNc is indicated **(D)** as the absolute number of TH-positive cells in the nonlesioned and lesioned hemisphere and **(E)** as the percentage of surviving neurons in the lesioned SNc compared with the intact SNc. Abbreviations: 6-OHDA, 6-hydroxydopamine; rMSC, rat mesenchymal stem cell; SNc, substantia nigra pars compacta; TH, tyrosine hydroxylase.

Distribution of Infused rMSCs in the Brain

Co-labeling with CellVue NIR815 (green signal) and PKH26 (red signal) allowed us to map the distribution of infused rMSCs in the brain (supplemental online Fig. 3). In the absence of mannitol pretreatment, only a paltry amount (Fig. 6A) of infused rMSCs were found in the brain. The number of infused cells was significantly higher in the presence of mannitol pretreatment, at 7 days postinfusion, deploying along the entire rostrocaudal axis and remaining substantially stable at the 28th day (Fig. 6A). Infused rMSCs spread to both hemispheres, although they tended to preferentially localize in the right hemisphere, ipsilaterally to the intracarotid infusion (Fig. 6B, 6C). This tendency was particularly evident at the seventh day postinfusion, when cells were mainly localized in the cortical areas of the right hemisphere (Fig. 7), confirming the speckled NIR fluorescent signal shown by ex vivo analysis. Differently, in the left hemisphere, rMSCs were mostly distributed in the subcortical regions and across the corpus callosum. Microscopic analysis of midbrain and hindbrain regions indicated a scattered distribution of infused rMSCs in these brain areas. This pattern of cell distribution was substantially maintained also at 28 days postinfusion, although an increase in the percentage of rMSCs localizing within the striatum and SNc, compared with day 7, was observed (Fig. 6C).

It is noteworthy that at 7 days after infusion, the infused cells were mainly found in blood vessels, whereas only rare cells were located in the brain parenchyma. Many rMSCs in blood vessels had a fusiform shape and tended to adhere to the wall of the vessel, suggesting a cell attempt to transmigrate into the parenchyma [61]. Accordingly, at 28 days after infusion, the great majority of rMSCs were found in the brain parenchyma.

DISCUSSION

Bone marrow-derived MSCs, or hematopoietic stem cells, are the only stem cells tested so far in patients with typical [35, 36, 39] or atypical degenerative parkinsonism [37, 38]. Modest beneficial effects on symptoms and disease progression have been reported, but crucial questions have remained unanswered. In particular, since MSCs were infused systemically in most cases, whether cells actually reached the brain parenchyma and engrafted at injured sites, to exert their therapeutic effects, remained an open issue.

To address this issue, we investigated the fate of rMSCs following intracarotid infusion in a 6-OHDA animal model of PD. Since crossing the BBB is crucial for the potential application of MSCs in treating neurological diseases, the rMSC infusion was performed with and without pretreatment with mannitol, a BBB permeabilizing agent, to verify if transient BBB opening could improve cell delivery to the brain. The distribution of infused cells to peripheral organs was also examined, as this aspect should be taken into consideration, as well, with a view to therapeutic application in
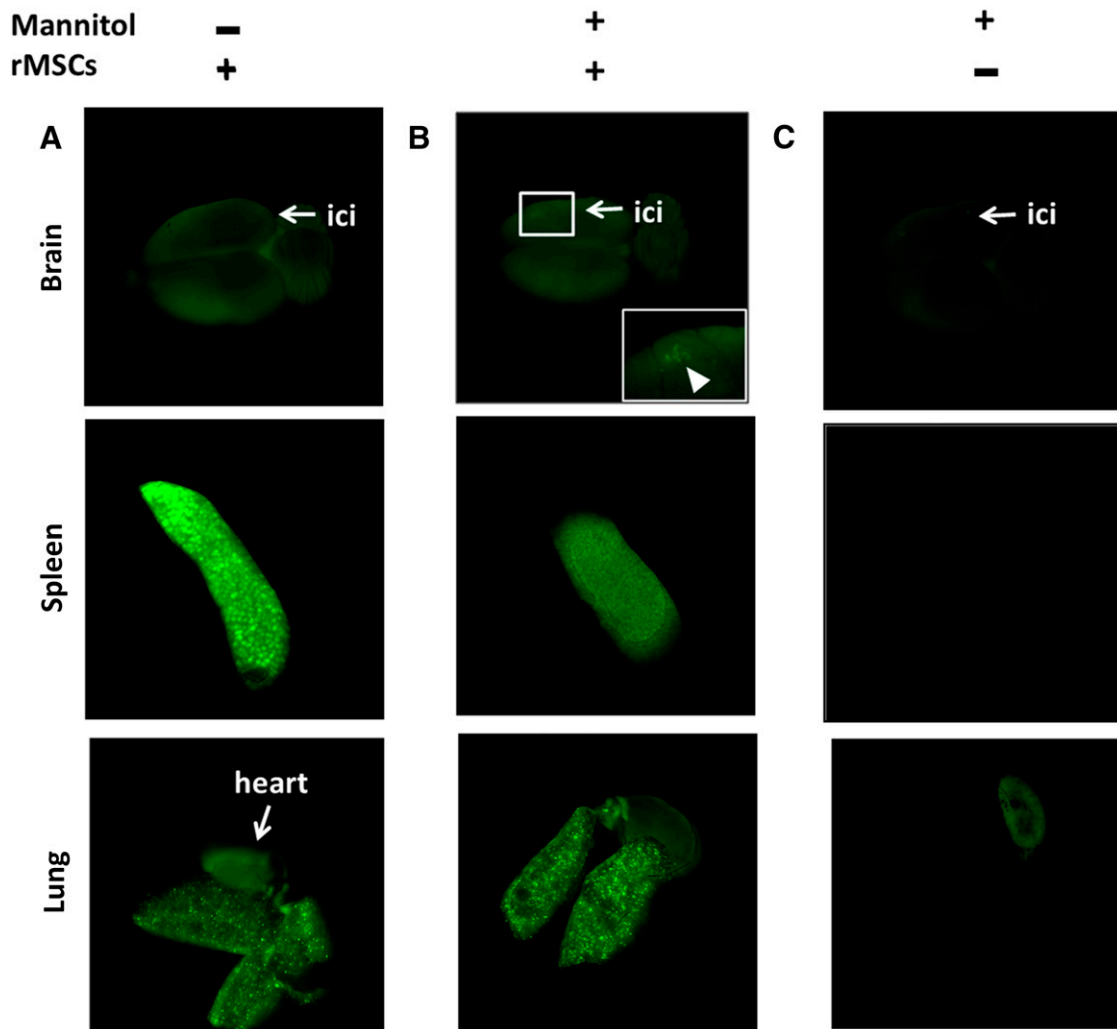
Figure 5. Whole-body distribution of rMSCs in the intrastriatal 6-OHDA rat model. At the moment of sacrifice, peripheral organs were excised and underwent near-IR imaging to evaluate the distribution of NIR815-positive rMSCs. **(A):** In the absence of mannitol treatment, no remarkable rMSC signal is detected into the brain of 6-OHDA animals. **(B):** A speckled NIR815-positive signal (arrowhead) is visible within the brain parenchyma ipsilateral to the ici, in the animal group that underwent transient blood-brain barrier disruption. **(C):** Negative control (no rMSC infusion). Unlike the brain, lung and spleen of rats receiving rMSCs, with **(B)** or without **(A)** mannitol pretreatment, show an intense NIR signal. Images represent the actual size of the organs and are equally representative of both time points chosen (7 and 28 days) after cell infusion. Bright green signal, NIR815. Abbreviations: 6-OHDA, 6-hydroxydopamine; ici, intracarotid infusion; NIR, near-infrared; NIR815, near-infrared 815-nm spectrum; rMSC, rat mesenchymal stem cell.

humans. We also investigated the effects of intraarterial infusion of rMSCs on the progression of nigrostriatal degeneration and motor deficits induced by 6-OHDA injection.

Effects of Mannitol on rMSC Delivery to the Brain

Mannitol is used in clinical practice for the management of intracranial hypertension [62] and to maximize the delivery of chemotherapeutic agents to the brain in the treatment of patients with cerebral tumors [43], thanks to its permeabilizing effect on the BBB. In our study, pretreatment with hyperosmolar mannitol substantially increased passage of infused rMSCs into the brain parenchyma, thereby confirming the results obtained in animal models of traumatic brain injury [45] and intracerebral hemorrhage [44].

Cell Distribution After Intracarotid Infusion

Numerous in vivo studies have shown that MSCs could migrate to injured, inflamed tissues from blood [63, 64], possibly in response to chemokines, cytokines, and growth factors released at the site of injury [61, 65]. In animal models of stroke, infused cells were mainly distributed in the ischemic hemisphere and were concentrated around the infarct region [66–68]. In our animals, rMSCs were scattered along the rostrocaudal brain axis; localization at the lesion sites (i.e., striatum and SNc) was limited, although it tended to increase over time. Infused rMSCs tended to preferentially localize in the hemisphere ipsilateral to the intracarotid infusion, but they were also found in the contralateral hemisphere, where their concentration increased at the later stage. This may suggest that the tendency of rMSCs to concentrate in the lesioned hemisphere was more likely due to the mannitol-induced transient BBB opening in this side rather than to a chemotactic attraction exerted by lesion. The distribution pattern was similar to that observed in animal models of stroke following local or systemic administration of MSCs [68, 69] and reflects the migratory ability of these cells. The presence of rMSC clusters along the corpus callosum—a preferential migration
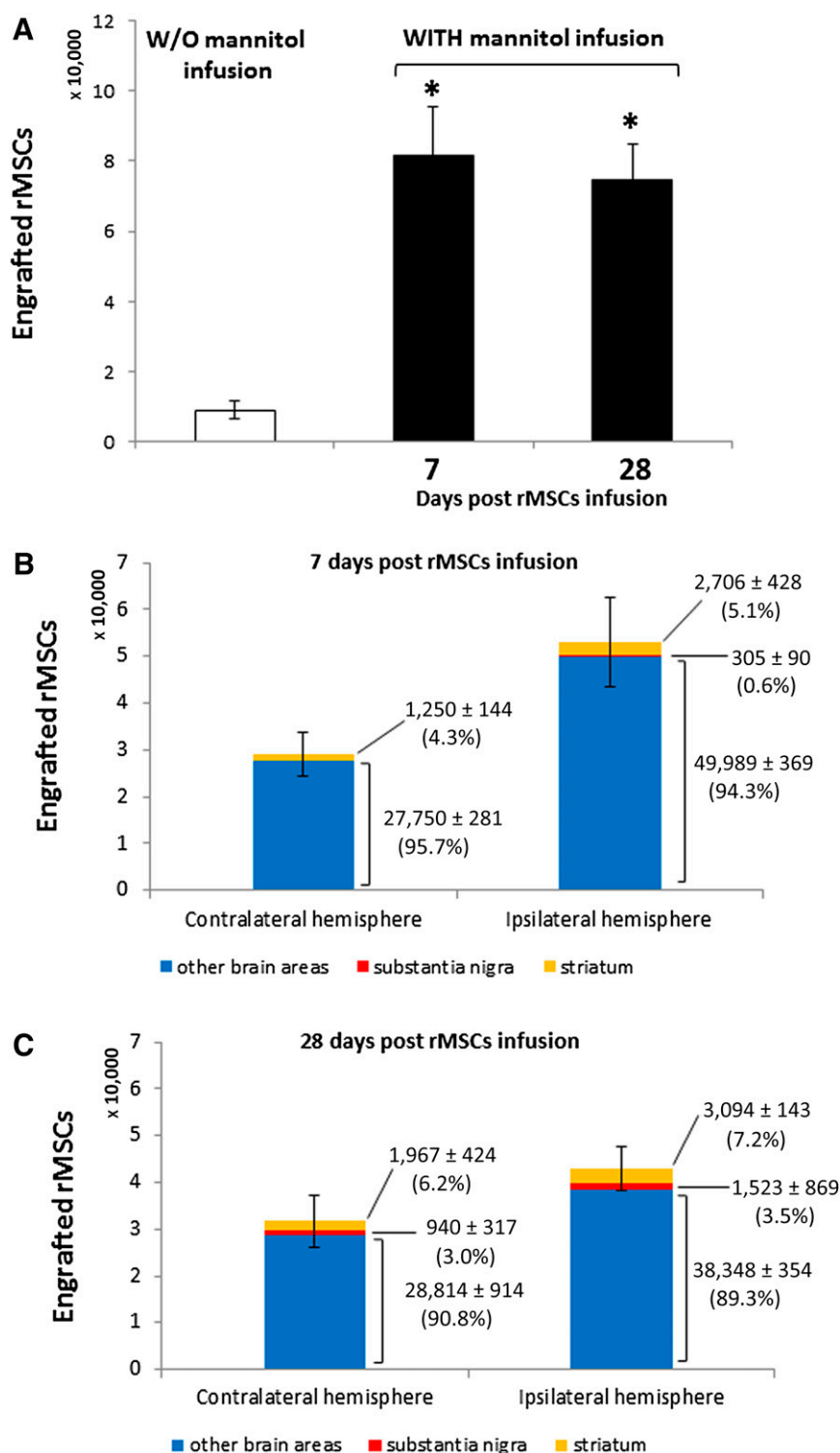
Figure 6. Quantitative analysis of rMSC distribution in the brain of 6-hydroxydopamine rat model. Seven and 28 days after rMSC infusion, tissue sections of the brain were examined under a fluorescent microscope and cells were counted along the entire rostrocaudal axis, in both hemispheres. **(A):** Mannitol pretreatment significantly enhanced the passage of rMSCs across the blood-brain barrier. Results (mean ± SEM) represent the estimated absolute number of the rMSCs engrafted into the brain. **(B, C):** In the animals pretreated with mannitol, infused rMSCs spread to both hemispheres, although they preferentially localized in the hemisphere ipsilateral to the intracarotid infusion. This tendency was more evident at 7 days after infusion, and slightly reduced over time. Bar graphs show the distribution of cells within striatum and substantia nigra in both hemispheres; both the estimated absolute number and the percentage of engrafted cells with respect of total cells infused (in brackets) were reported. ∗, $p < .05$ Kruskal-Wallis test versus W/O mannitol infusion. Abbreviations: 6-OHDA, 6-hydroxydopamine; rMSC, rat mesenchymal stem cell; W/O, without.
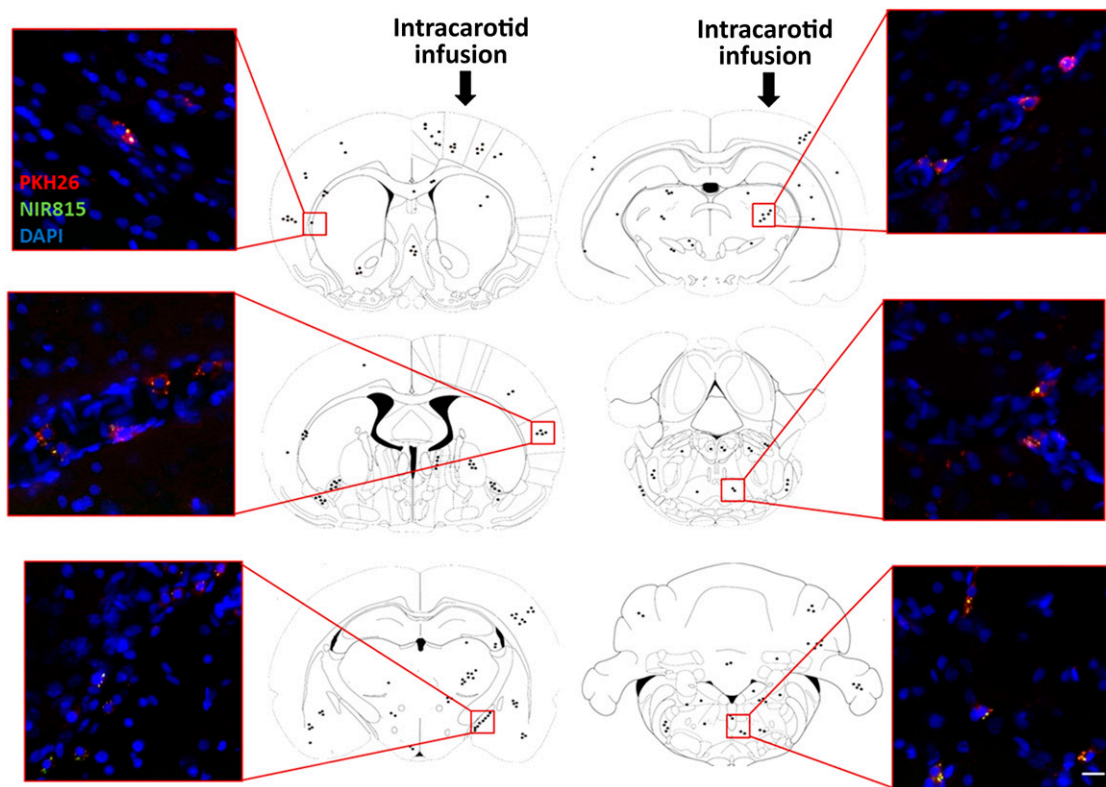
Figure 7. Central distribution of rat mesenchymal stem cells (rMSCs) in the intrastriatal 6-hydroxydopamine rat model. Tissue sections of the brain were examined under a fluorescent microscope for tracking cell distribution along the entire rostrocaudal axis, in both hemispheres. The figure shows a graphical representation of cell distribution in the animal group pretreated with mannitol, at 7 days after rMSC infusion. Infused rMSCs showed a scattered arrangement in both hemispheres, with a prevailing tendency to localize in the hemisphere ipsilateral to the intra-carotid infusion, especially in the forebrain. Red signal, PKH26; bright green signal, NIR815; blue signal, DAPI. Scale bar: 20 μm. Abbreviation: DAPI, 4',6-diamidino-2-phenylindole; NIR815, near-infrared 815-nm spectrum.

route of stem cells [70–72]—in the short term after infusion further confirms this observation.

At day 7 postinfusion, we detected rMSCs mainly in cerebral blood vessels. The persistence of MSCs within blood vessels, even several days after the infusion, has already been reported [69, 73]. Although the homing mechanism is still incompletely understood, to leave the bloodstream, MSCs may use the same sequential mechanism adopted by lymphocytes and hematopoietic stem cells, which roll along the vascular endothelium and, at some point, encounter chemokine-activated integrins that prompt arrest of the cells and their subsequent transendothelial migration [74]. Therefore, the predominant presence of rMSCs within blood vessels at day 7 postinfusion could be the step that precedes their transmigration through the vessel wall. This hypothesis is supported by the increasing localization of infused cells in the brain parenchyma, rather than in the blood circulation, detectable at day 28 postinfusion.

A striking finding of our study was the remarkable rMSC accumulation in peripheral organs. We were expecting the intraarterial route of administration to favor brain penetration of MSCs and substantially reduce their accumulation within filtering organs (i.e., lungs, liver, spleen) compared with intravenous delivery [75, 76]. However, we detected a strong rMSC signal in the lungs and spleen up to 28 days after infusion. We cannot exclude that this may be a temporary condition, especially for lung entrapment. Indeed, studies using intravenous MSC administration showed that, after an initial concentration in the lungs, the injected cells could gradually migrate to sites of injury [76–78].

Effects of rMSC Infusion on 6-OHDA-Induced Neurodegeneration and Motor Deficits

In most studies conducted in experimental PD models, MSCs were directly injected into the nigrostriatal system. These studies showed positive effects in terms of neuroprotection and improvement of motor deficits [13, 15, 17], even if several of these works used genetically modified or neural-induced MSCs [79–82]. We have previously demonstrated that striatal grafts of undifferentiated human MSCs increase the survival of cell bodies and terminals of dopaminergic nigrostriatal neurons, coupled with a reduction of the apomorphine-induced turning behavior associated with the lesion [14]. In the present study, however, intracarotid infusion of rMSCs did not affect the progression of 6-OHDA-induced neurodegeneration, nor was forelimb akinesia improved, as assessed by the stepping test. One possible, and obvious, explanation for this discrepancy is that the number of cells reaching the brain—and the injury sites, in particular—may have been too small to exert a neuroprotective effect. Indeed, although pretreatment with mannitol significantly enhanced rMSC delivery into the brain, cell concentration at the injury sites was still incomparably smaller than the concentration achieved with the intracerebral graft.

An unexpected result, given the inefficacy of the intracarotid infusion of rMSC on the nigrostriatal lesion and forelimb akinesia induced by 6-OHDA, was the striking modification of the apomorphine-induced turning behavior. Contralateral turning

in response to apomorphine administration is classically considered an index of striatal dopaminergic denervation in rodents with unilateral nigrostriatal lesion. This motor behavior was abolished in the animals that received the rMSCs infusion, being substituted by moderate ipsilateral turning at the first week postinfusion and totally disappearing at the fourth week. This was the most puzzling finding of this study. The loss of striatal dopamine caused by 6-OHDA triggers supersensitivity of striatal dopaminergic receptors within the denervated striatum; this mechanism is responsible for the asymmetrical response to the dopamine agonist apomorphine, which ultimately forces the animal to rotate contralaterally to the lesioned hemisphere [83]. Dopaminergic stimulation triggers the expression of c-Fos, a marker of neuronal activation, in striatal neurons of rats bearing a nigrostriatal lesion [84]. Accordingly, the rotational response to apomorphine observed in untreated lesioned animals was associated with more c-Fos-positive neurons within the denervated striatum and negligible c-Fos expression in the intact striatum. Interestingly, disappearance of the turning behavior in rMSC-treated lesioned animals, at the fourth week postinfusion, was associated with increased c-Fos expression in the intact striatum, while no changes were detected in the lesioned side. Therefore, it appears that, rather than affecting the dopaminergic supersensitivity of striatal neurons of the lesioned side, cell treatment enhanced the response to apomorphine in the intact side. This may have translated in restoration of the functional balance between the two striata, causing disappearance of the rotational behavior.

A potential explanation for this phenomenon may involve the recognized ability of rMSCs to secrete regulatory and trophic factors. Brain-derived neurotrophic factor (BDNF), in particular, is constitutively synthesized and released by MSCs, which maintain this ability after transplantation [14, 29, 85, 86]. BDNF is a key regulator of neural circuit function and is involved in the modulation of synaptic function by changing either the efficacy of presynaptic transmitter release or the magnitude of postsynaptic responses [87]. The biological effects of BDNF are primarily mediated by TrkB receptors, which are abundantly expressed in striatal neurons. McGinty et al. [88] suggested a functional interaction between the intracellular signaling cascades activated by dopamine D1 and TrkB receptors in these neurons, which would influence the behavioral and neurochemical responses to dopaminergic stimulation. Therefore, as we observed substantial migration of rMSCs to the unlesioned hemisphere, it is possible that BDNF released from rMSCs enhanced the response to apomorphine in the intact striatum. The absence of such effect in the lesioned side may be due to the fact that the responsiveness of striatal neurons was already saturated, due to the dopaminergic supersensitvity. This is in keeping with the data reported by Berg et al. [13], who detected increased levels of BDNF mRNA in the intact hemisphere, but not in the lesioned one, of 6-OHDA injected rats that had received intranigral transplantation of adherent MSCs isolated from human adipose tissue; also in this case, no reversal of 6-OHDA-induced neurotoxicity was observed, while turning behavior was reduced. Moreover, adenoviral-mediated expression of BDNF in the substantia nigra and striatum of 6-OHDA-lesioned animals improved rotational behavior without exerting actual neuroprotective effects. This discrepancy was attributed to the fact that higher BDNF levels were probably required to protect nigrostriatal neurons [89, 90]. Analogously, it is likely that the low number of rMSCs reaching the injury sites following intracarotid infusion may release BDNF at levels that are sufficient to interfere with dopaminergic transmission, but not to exert neurorestorative effects. Finally, regarding the apparent discrepancy regarding the inefficacy of rMSC infusion on forelimb akinesia (stepping test), previous studies have pointed out that rotational behavior and skilled movements are differently affected in rats bearing a 6-OHDA-induced lesion of the nigrostriatal tract [91–94], implying that treatments reducing turning behavior will not necessarily lead to parallel improvements in skilled motor function.

CONCLUSION

Our work shows that appreciable delivery of rMSCs to the brain of 6-OHDA-lesioned animals can be obtained only after mannitol pretreatment, indicating that the use of a permeabilizing agent is essential to allow passage of rMSCs across the BBB. A notable percentage of infused cells accumulated in the peripheral organs. Infusion of rMSCs did not modify the progression of 6-OHDA-induced damage in the striatum or SNc, but profoundly affected the behavioral stereotypies triggered by apomorphine. This suggests that arterially infused MSCs may induce functional compensatory changes in the nigrostriatal system by modulating the responsiveness of striatal neurons to dopaminergic stimulation. Future investigations should further explore this capability of MSCs, while neuroprotective or neurorestorative effects, at least under these experimental conditions, can be excluded.

ACKNOWLEDGMENT

AUTHOR CONTRIBUTIONS

S.C. and R.G.: conception and design, collection and assembly of data, data analysis and interpretation, and manuscript writing; G.L. and C.G.: conception and design, collection and assembly of data, data analysis and interpretation; A.S.M., M.A.A., and R.M.: collection and assembly of data, and data analysis and interpretation; M.-T.F.-A.: conception and design, data analysis and interpretation; A.B.: collection and assembly of data; F.B.: conception and design, financial support, data analysis and interpretation, manuscript writing and final approval of manuscript.

DISCLOSURE OF POTENTIAL CONFLICTS OF INTEREST

The authors indicated no potential conflicts of interest.

REFERENCES

1 Defer GL, Geny C, Ricolfi F et al. Long-term outcome of unilaterally transplanted parkinsonian patients. I. Clinical approach. Brain 1996;119:41–50.

2 Freed CR, Breeze RE, Rosenberg NL et al. Survival of implanted fetal dopamine cells and neurologic improvement 12 to 46 months after transplantation for Parkinson's disease. N Engl J Med 1992;327:1549–1555.

3 Lindvall O, Brundin P, Widner H et al. Grafts of fetal dopamine neurons survive and improve motor function in Parkinson's disease. Science 1990;247:574–577.

4 Madrazo I, León V, Torres C et al. Transplantation of fetal substantia nigra and adrenal medulla to the caudate nucleus in two patients with Parkinson's disease. N Engl J Med 1988; 318:51.

5 Björklund LM, Sánchez-Pernaute R, Chung S et al. Embryonic stem cells develop into

functional dopaminergic neurons after transplantation in a Parkinson rat model. Proc Natl Acad Sci USA 2002;99:2344–2349.

6   Cho YH, Kim DS, Kim PG et al. Dopamine neurons derived from embryonic stem cells efficiently induce behavioral recovery in a Parkinsonian rat model. Biochem Biophys Res Commun 2006;341:6–12.

7   Takagi Y, Takahashi J, Saiki H et al. Dopaminergic neurons generated from monkey embryonic stem cells function in a Parkinson primate model. J Clin Invest 2005;115:102–109.

8   Snyder BJ, Olanow CW. Stem cell treatment for Parkinson's disease: An update for 2005. Curr Opin Neurol 2005;18:376–385.

9   Hargus G, Cooper O, Deleidi M et al. Differentiated Parkinson patient-derived induced pluripotent stem cells grow in the adult rodent brain and reduce motor asymmetry in Parkinsonian rats. Proc Natl Acad Sci USA 2010;107:15921–15926.

10   Rhee YH, Ko JY, Chang MY et al. Protein-based human iPS cells efficiently generate functional dopamine neurons and can treat a rat model of Parkinson disease. J Clin Invest 2011;121:2326–2335.

11   Wernig M, Zhao JP, Pruszak J et al. Neurons derived from reprogrammed fibroblasts functionally integrate into the fetal brain and improve symptoms of rats with Parkinson's disease. Proc Natl Acad Sci USA 2008;105:5856–5861.

12   Ahmed H, Salem A, Atta H et al. Do adipose tissue-derived mesenchymal stem cells ameliorate Parkinson's disease in rat model? Hum Exp Toxicol 2014;33:1217–1231.

13   Berg J, Roch M, Altschüler J et al. Human adipose-derived mesenchymal stem cells improve motor functions and are neuroprotective in the 6-hydroxydopamine-rat model for Parkinson's disease when cultured in monolayer cultures but suppress hippocampal neurogenesis and hippocampal memory function when cultured in spheroids. Stem Cell Rev 2015;11:133–149.

14   Blandini F, Cova L, Armentero MT et al. Transplantation of undifferentiated human mesenchymal stem cells protects against 6-hydroxydopamine neurotoxicity in the rat. Cell Transplant 2010;19:203–217.

15   Bouchez G, Sensebé L, Vourc'h P et al. Partial recovery of dopaminergic pathway after graft of adult mesenchymal stem cells in a rat model of Parkinson's disease. Neurochem Int 2008;52:1332–1342.

16   Capitelli CS, Lopes CS, Alves AC et al. Opposite effects of bone marrow-derived cells transplantation in MPTP-rat model of Parkinson's disease: A comparison study of mononuclear and mesenchymal stem cells. Int J Med Sci 2014;11:1049–1064.

17   Chao YX, He BP, Tay SS. Mesenchymal stem cell transplantation attenuates blood brain barrier damage and neuroinflammation and protects dopaminergic neurons against MPTP toxicity in the substantia nigra in a model of Parkinson's disease. J Neuroimmunol 2009;216:39–50.

18   Kim YJ, Park HJ, Lee G et al. Neuroprotective effects of human mesenchymal stem cells on dopaminergic neurons through anti-inflammatory action. Glia 2009;57:13–23.

19   Park HJ, Lee PH, Bang OY et al. Mesenchymal stem cells therapy exerts neuroprotection in a progressive animal model of Parkinson's disease. J Neurochem 2008;107:141–151.

20   Park HJ, Shin JY, Kim HN et al. Neuroprotective effects of mesenchymal stem cells through autophagy modulation in a parkinsonian model. Neurobiol Aging 2014;35:1920–1928.

21   Sadan O, Bahat-Stromza M, Barhum Y et al. Protective effects of neurotrophic factor-secreting cells in a 6-OHDA rat model of Parkinson disease. Stem Cells Dev 2009;18:1179–1190.

22   Suzuki S, Kawamata J, Iwahara N et al. Intravenous mesenchymal stem cell administration exhibits therapeutic effects against 6-hydroxydopamine-induced dopaminergic neurodegeneration and glial activation in rats. Neurosci Lett 2015;584:276–281.

23   Krampera M, Pasini A, Pizzolo G et al. Regenerative and immunomodulatory potential of mesenchymal stem cells. Curr Opin Pharmacol 2006;6:435–441.

24   Barkholt L, Flory E, Jekerle V et al. Risk of tumorigenicity in mesenchymal stromal cell-based therapies—bridging scientific observations and regulatory viewpoints. Cytotherapy 2013;15:753–759.

25   Bernardo ME, Zaffaroni N, Novara F et al. Human bone marrow derived mesenchymal stem cells do not undergo transformation after long-term in vitro culture and do not exhibit telomere maintenance mechanisms. Cancer Res 2007;67:9142–9149.

26   Choumerianou DM, Dimitriou H, Perdikogianni C et al. Study of oncogenic transformation in ex vivo expanded mesenchymal cells, from paediatric bone marrow. Cell Prolif 2008;41:909–922.

27   de Girolamo L, Lucarelli E, Alessandri G et al. Mesenchymal stem/stromal cells: A new "cells as drugs" paradigm. Efficacy and critical aspects in cell therapy. Curr Pharm Des 2013;19:2459–2473.

28   von Bahr L, Batsis I, Moll G et al. Analysis of tissues following mesenchymal stromal cell therapy in humans indicates limited long-term engraftment and no ectopic tissue formation. STEM CELLS 2012;30:1575–1578.

29   Cova L, Armentero MT, Zennaro E et al. Multiple neurogenic and neurorescue effects of human mesenchymal stem cell after transplantation in an experimental model of Parkinson's disease. Brain Res 2010;1311:12–27.

30   Crigler L, Robey RC, Asawachaicharn A et al. Human mesenchymal stem cell subpopulations express a variety of neuro-regulatory molecules and promote neuronal cell survival and neuritogenesis. Exp Neurol 2006;198:54–64.

31   Kan I, Barhum Y, Melamed E et al. Mesenchymal stem cells stimulate endogenous neurogenesis in the subventricular zone of adult mice. Stem Cell Rev 2011;7:404–412.

32   Paul G, Anisimov SV. The secretome of mesenchymal stem cells: potential implications for neuroregeneration. Biochimie 2013;95:2246–2256.

33   Shi Y, Su J, Roberts AI et al. How mesenchymal stem cells interact with tissue immune responses. Trends Immunol 2012;33:136–143.

34   Tfilin M, Sudai E, Merenlender A et al. Mesenchymal stem cells increase hippocampal neurogenesis and counteract depressive-like behavior. Mol Psychiatry 2010;15:1164–1175.

35   Venkataramana NK, Kumar SK, Balaraju S et al. Open-labeled study of unilateral autologous bone-marrow-derived mesenchymal stem cell transplantation in Parkinson's disease. Transl Res 2010;155:62–70.

36   Venkataramana NK, Pal R, Rao SA et al. Bilateral transplantation of allogenic adult human bone marrow-derived mesenchymal stem cells into the subventricular zone of Parkinson's disease: A pilot clinical study. Stem Cells Int 2012;2012:931902.

37   Lee PH, Kim JW, Bang OY et al. Autologous mesenchymal stem cell therapy delays the progression of neurological deficits in patients with multiple system atrophy. Clin Pharmacol Ther 2008;83:723–730.

38   Lee PH, Lee JE, Kim HS et al. A randomized trial of mesenchymal stem cells in multiple system atrophy. Ann Neurol 2012;72:32–40.

39   Brazzini A, Cantella R, De la Cruz A et al. Intraarterial autologous implantation of adult stem cells for patients with Parkinson disease. J Vasc Interv Radiol 2010;21:443–451.

40   Carvey PM, Zhao CH, Hendey B et al. 6-Hydroxydopamine-induced alterations in blood-brain barrier permeability. Eur J Neurosci 2005;22:1158–1168.

41   Kortekaas R, Leenders KL, van Oostrom JC et al. Blood-brain barrier dysfunction in parkinsonian midbrain in vivo. Ann Neurol 2005;57:176–179.

42   Pisani V, Stefani A, Pierantozzi M et al. Increased blood-cerebrospinal fluid transfer of albumin in advanced Parkinson's disease. J Neuroinflammation 2012;9:188.

43   Bellavance MA, Blanchette M, Fortin D. Recent advances in blood-brain barrier disruption as a CNS delivery strategy. AAPS J 2008;10:166–177.

44   Seyfried DM, Han Y, Yang D et al. Mannitol enhances delivery of marrow stromal cells to the brain after experimental intracerebral hemorrhage. Brain Res 2008;1224:12–19.

45   Okuma Y, Wang F, Toyoshima A et al. Mannitol enhances therapeutic effects of intra-arterial transplantation of mesenchymal stem cells into the brain after traumatic brain injury. Neurosci Lett 2013;554:156–161.

46   Blandini F, Levandis G, Bazzini E et al. Time-course of nigrostriatal damage, basal ganglia metabolic changes and behavioural alterations following intrastriatal injection of 6-hydroxydopamine in the rat: new clues from an old model. Eur J Neurosci 2007;25:397–405.

47   Paxinos G, Watson C. The Rat Brain in Stereotaxic Coordinates. 7th ed.San Diego, CA: Academic Press, 1998.

48   Colaianna M, Tucci P, Zotti M et al. Soluble beta amyloid(1-42): A critical player in producing behavioural and biochemical changes evoking depressive-related state? Br J Pharmacol 2010;159:1704–1715.

49   Rapoport SI, Fredericks WR, Ohno K et al. Quantitative aspects of reversible osmotic opening of the blood-brain barrier. Am J Physiol 1980;238:R421–R431.

50   Cosolo WC, Martinello P, Louis WJ et al. Blood-brain barrier disruption using mannitol: time course and electron microscopy studies. Am J Physiol 1989;256:R443–R447.

51   Blanchette M, Fortin D. Blood-brain barrier disruption in the treatment of brain tumors. Methods Mol Biol 2011;686:447–463.

52 Al-Mehdi AB, Patel M, Haroon A et al. Increased depth of cellular imaging in the intact lung using far red and near infrared fluorescent probes. Int J Biomed Imag 2006;2006:37470.

53 Bossolasco P, Cova L, Levandis G et al. Noninvasive near-infrared live imaging of human adult mesenchymal stem cells transplanted in a rodent model of Parkinson's disease. Int J Nanomedicine 2012;7:435–447.

54 Hanabusa K, Nagaya N, Iwase T et al. Adrenomedullin enhances therapeutic potency of mesenchymal stem cells after experimental stroke in rats. Stroke 2005;36:853–858.

55 Lehner T, Mitchell E, Bergmeier L et al. The role of gammadelta T cells in generating antiviral factors and beta-chemokines in protection against mucosal simian immunodeficiency virus infection. Eur J Immunol 2000;30:2245–2256.

56 Morigi M, Rota C, Montemurro T et al. Life-sparing effect of human cord blood-mesenchymal stem cells in experimental acute kidney injury. STEM CELLS 2010;28:513–522.

57 Wallace PK, Muirhead KA. Cell tracking 2007: A proliferation of probes and applications. Immunol Invest 2007;36:527–561.

58 Olsson M, Nikkhah G, Bentlage C et al. Forelimb akinesia in the rat Parkinson model: differential effects of dopamine agonists and nigral transplants as assessed by a new stepping test. J Neurosci 1995;15:3863–3875.

59 Tassorelli C, Armentero MT, Greco R et al. Behavioral responses and Fos activation following painful stimuli in a rodent model of Parkinson's disease. Brain Res 2007;1176:53–61.

60 West MJ, Slomianka L, Gundersen HJ. Unbiased stereological estimation of the total number of neurons in the subdivisions of the rat hippocampus using the optical fractionator. Anat Rec 1991;231:482–497.

61 Kholodenko IV, Konieva AA, Kholodenko RV et al. Molecular mechanisms of migration and homing of intravenously transplanted mesenchymal stem cells. J Regen Med Tissue Eng 2013.

62 Shawkat H, Westwood MM, Mortimer A. Mannitol: a review of its clinical uses. Contin Educ Anaesth Crit Care Pain 2012;2:82–85.

63 Chapel A, Bertho JM, Bensidhoum M et al. Mesenchymal stem cells home to injured tissues when co-infused with hematopoietic cells to treat a radiation-induced multi-organ failure syndrome. J Gene Med 2003;5:1028–1038.

64 Chavakis E, Urbich C, Dimmeler S. Homing and engraftment of progenitor cells: a prerequisite for cell therapy. J Mol Cell Cardiol 2008;45:514–522.

65 Shen LH, Li Y, Chen J et al. Therapeutic benefit of bone marrow stromal cells administered 1 month after stroke. J Cereb Blood Flow Metab 2007;27:6–13.

66 Gutiérrez-Fernández M, Rodríguez-Frutos B, Alvarez-Grech J et al. Functional recovery after hematic administration of allogenic mesenchymal stem cells in acute ischemic stroke in rats. Neuroscience 2011;175:394–405.

67 Lu SS, Liu S, Zu QQ et al. In vivo MR imaging of intraarterially delivered magnetically labeled mesenchymal stem cells in a canine stroke model. PLoS One 2013;8:e54963.

68 Ruan GP, Han YB, Wang TH et al. Comparative study among three different methods of bone marrow mesenchymal stem cell transplantation following cerebral infarction in rats. Neurol Res 2013;35:212–220.

69 Pavlichenko N, Sokolova I, Vijde S et al. Mesenchymal stem cells transplantation could be beneficial for treatment of experimental ischemic stroke in rats. Brain Res 2008;1233:203–213.

70 Hoehn M, Küstermann E, Blunk J et al. Monitoring of implanted stem cell migration in vivo: a highly resolved in vivo magnetic resonance imaging investigation of experimental stroke in rat. Proc Natl Acad Sci USA 2002;99:16267–16272.

71 Jackson JS, Golding JP, Chapon C et al. Homing of stem cells to sites of inflammatory brain injury after intracerebral and intravenous administration: A longitudinal imaging study. Stem Cell Res Ther 2010;1:17.

72 Modo M, Mellodew K, Cash D et al. Mapping transplanted stem cell migration after a stroke: a serial, in vivo magnetic resonance imaging study. Neuroimage 2004;21:311–317.

73 Walczak P, Zhang J, Gilad AA et al. Dual-modality monitoring of targeted intraarterial delivery of mesenchymal stem cells after transient ischemia. Stroke 2008;39:1569–1574.

74 Springer TA. Traffic signals for lymphocyte recirculation and leukocyte emigration: the multistep paradigm. Cell 1994;76:301–314.

75 Barbash IM, Chouraqui P, Baron J et al. Systemic delivery of bone marrow-derived mesenchymal stem cells to the infarcted myocardium: Feasibility, cell migration, and body distribution. Circulation 2003;108:863–868.

76 Kraitchman DL, Tatsumi M, Gilson WD et al. Dynamic imaging of allogeneic mesenchymal stem cells trafficking to myocardial infarction. Circulation 2005;112:1451–1461.

77 Deak E, Seifried E, Henschler R. Homing pathways of mesenchymal stromal cells (MSCs) and their role in clinical applications. Int Rev Immunol 2010;29:514–529.

78 Lee RH, Pulin AA, Seo MJ et al. Intravenous hMSCs improve myocardial infarction in mice because cells embolized in lung are activated to secrete the anti-inflammatory protein TSG-6. Cell Stem Cell 2009;5:54–63.

79 Levy YS, Bahat-Stroomza M, Barzilay R et al. Regenerative effect of neural-induced human mesenchymal stromal cells in rat models of Parkinson's disease. Cytotherapy 2008;10:340–352.

80 Lu L, Zhao C, Liu Y et al. Therapeutic benefit of TH-engineered mesenchymal stem cells for Parkinson's disease. Brain Res Brain Res Protoc 2005;15:46–51.

81 Yan M, Sun M, Zhou Y et al. Conversion of human umbilical cord mesenchymal stem cells in Wharton's jelly to dopamine neurons mediated by the Lmx1a and neurturin in vitro:

potential therapeutic application for Parkinson's disease in a rhesus monkey model. PLoS One 2013;8:e64000.

82 Park S, Kim E, Koh SE et al. Dopaminergic differentiation of neural progenitors derived from placental mesenchymal stem cells in the brains of Parkinson's disease model rats and alleviation of asymmetric rotational behavior. Brain Res 2012;1466:158–166.

83 Schwarting RK, Huston JP. The unilateral 6-hydroxydopamine lesion model in behavioral brain research. Analysis of functional deficits, recovery and treatments. Prog Neurobiol 1996;50:275–331.

84 Labandeira-Garcia JL, Rozas G, Lopez-Martin E et al. Time course of striatal changes induced by 6-hydroxydopamine lesion of the nigrostriatal pathway, as studied by combined evaluation of rotational behaviour and striatal Fos expression. Exp Brain Res 1996;108:69–84.

85 Harper MM, Grozdanic SD, Blits B et al. Transplantation of BDNF-secreting mesenchymal stem cells provides neuroprotection in chronically hypertensive rat eyes. Invest Ophthalmol Vis Sci 2011;52:4506–4515.

86 Zhao HB, Ma H, Ha XQ et al. Salidroside induces rat mesenchymal stem cells to differentiate into dopaminergic neurons. Cell Biol Int 2014;38:462–471.

87 Park H, Poo MM. Neurotrophin regulation of neural circuit development and function. Nat Rev Neurosci 2013;14:7–23.

88 McGinty JF, Bache AJ, Coleman NT et al. The role of BDNF/TrkB signaling in acute amphetamine-induced locomotor activity and opioid peptide gene expression in the rat dorsal striatum. Front Syst Neurosci 2011;5:60.

89 Klein RL, Lewis MH, Muzyczka N et al. Prevention of 6-hydroxydopamine-induced rotational behavior by BDNF somatic gene transfer. Brain Res 1999;847:314–320.

90 Sun M, Kong L, Wang X et al. Comparison of the capability of GDNF, BDNF, or both, to protect nigrostriatal neurons in a rat model of Parkinson's disease. Brain Res 2005;1052:119–129.

91 Lee CS, Sauer H, Bjorklund A. Dopaminergic neuronal degeneration and motor impairments following axon terminal lesion by instrastriatal 6-hydroxydopamine in the rat. Neuroscience 1996;72:641–653.

92 Löscher W, Richter A, Nikkhah G et al. Behavioral and neurochemical dysfunction in the circling (ci) rat: a novel genetic animal model of a movement disorder. Neuroscience 1996;74:1135–1142.

93 Metz GA, Whishaw IQ. Drug-induced rotation intensity in unilateral dopamine-depleted rats is not correlated with end point or qualitative measures of forelimb or hindlimb motor performance. Neuroscience 2002;111:325–336.

94 Whishaw IQ, O'Connor WT, Dunnett SB. The contributions of motor cortex, nigrostriatal dopamine and caudate-putamen to skilled forelimb use in the rat. Brain 1986;109:805–843.

See www.StemCellsTM.com for supporting information available online.